https://doi.org/10.3311/PPme.44482

Periodica Polytechnica Mechanical Engineering

Determination of Biaxial Anisotropy Coefficient for LDX2205 Duplex Stainless Steel

Szabolcs Jónás[1*], Vilmos Nyáry[1], Levente Katula[1], Dorina Kovács[1]

[1] Department of Materials Science and Engineering, Faculty of Mechanical Engineering, Budapest University of Technology and Economics, Műegyetem rkp. 3., H-1111 Budapest, Hungary
[*] Corresponding author, e-mail: jonas.szabolcs@gpk.bme.hu

Received: 27 April 2026, Accepted: 04 June 2026, Published online: 16 June 2026

Abstract

In sheet metal forming processes such as deep drawing, planar anisotropy plays a crucial role in determining the final geometry. The formability of sheet metals depends on their anisotropic behavior; therefore, anisotropy can be a limitation of forming. Accurate finite element modeling of sheet metal forming processes requires a robust description of anisotropic behavior. The standardized approach for determining anisotropy is tensile testing at different angles relative to the sheet metal's rolling direction. Biaxial behavior is also important for the yield function of the materials. Although several methods are available for determining biaxial properties, the disk compression test is relatively simple and easy to perform and, therefore, a favorable method in an industrial environment. The goal of the present study is to determine the biaxial anisotropy coefficient of LDX2205 duplex stainless steel (DSS). Although the proper lubrication and the appropriate test methodology are unknown, a comparison is needed to define the methods and lubricants for further investigations. The tests were conducted with three lubricants to identify the most reliable one: a high-contact-pressure grease, a graphite-containing grease, and PTFE sheets. Based on measurements, the greatest deformation occurred when PTFE sheets were applied; therefore, further tests were performed using these sheets. Three series of compression tests were performed: a fully compressed series, a gradually compressed series, and a load-driven series. The investigations were carried out to examine the influence of the different methods on the parameter. Microhardness tests were conducted on the as-delivery-conditioned material and on the compressed material.

Keywords

disk compression, anisotropy, sheet metal

1 Introduction

In recent years, virtual manufacturing has come into focus in the industry due to the lower cost of high-performance computing compared to classical trial-and-error methodologies. The trend is to reduce testing of materials and structures and to use more numerical simulation data as input for faster, more efficient development [1]. Deep drawing is one of the most widely used metal-forming processes [2]. Numerical modeling of deep drawing processes is widely used in industry, and scientific research is also intensively pursued. Several research papers address modeling techniques and advanced material models to better predict material behavior [3, 4]. Barlat et al. [5] proposed the Yld2000-2d plane stress yield function that describes the anisotropic behavior of sheet metals, especially aluminum. An experiment was also introduced to obtain one of the anisotropy coefficients, r_b. The method is the disk compression test (DCT). DCT is a simple yet effective method for determining the r_b value; it can also be derived from other methods; however, its simplicity is beneficial given the available test equipment. Different authors used different diameters of specimens in their studies, e.g., Béres et al. [6] used 10 mm, Dick et al. [7] and Anderson et al. [8] used 12.7 mm, and Aretz et al. used 15 mm, but Martínez et al. [9] used 6.5 mm disks. In this study, the designated specimen diameter was set to 8 mm based on prior analytical calculations and the maximum load-bearing capacity of the material testing machine. To reduce friction, several greases, including oil, graphite, and PTFE, were used [5], [6], and [10]. Aretz and Barlat numerically analyzed the friction at the contacting surfaces. To properly measure the value of r_b, the most commonly applied procedure was to compress

Cite this article as: Jónás, S., Nyáry, V., Katula, L., Kovács, D. "Determination of Biaxial Anisotropy Coefficient for LDX2205 Duplex Stainless Steel", Periodica Polytechnica Mechanical Engineering, 2026. https://doi.org/10.3311/PPme.44482

a set of specimens, then measure the axes of the formed ellipses, and fit a line to the calculated strain values; however, Camberg and Tröster proposed a digital image correlation (DIC) method, which is more precise, but also more complex and expensive. [11].

The anisotropic behavior of the sheets during metal forming can be better described using this parameter, as shown by Tian et al. [12].

Numerous studies address the formability of DSS. For example, Mapelli et al. investigated symmetric and asymmetric hot-rolling processes [13], Reddy et al. examined incremental forming [14], and Rana et al. focused on the formability of DSS [15].

This research contributes to a better understanding of the formability of duplex steels and provides insights into modeling-related issues.

This research aims to identify the most suitable lubricant for conducting the tests and the most effective and reliable methodology for determining the biaxial anisotropy coefficient for LDX2205 duplex stainless steel.

2 Materials and methods

The test material was LDX2205 duplex stainless steel. This material was commonly used in harsh environments due to its unique microstructure. The ferritic-austenitic microstructure provides exceptional corrosion resistance [16]. Fig. 1 shows the microstructure of the examined material. The darker phase is the ferrite, and the lighter phase is the austenite. The chemical composition and mechanical properties of the investigated steel are shown in Tables 1 and 2, respectively.

The specimens were ground using 1200, 2500, and 4000 grit sandpaper, then polished with a 3-1 µm diamond suspension. The disks were etched by immersing them in a Beraha-type reagent solution (100 ml H_2O, 20 ml HCl, 1 g potassium metabisulfite) for 15 seconds at room temperature, then rinsed in water and dried [17, 18].

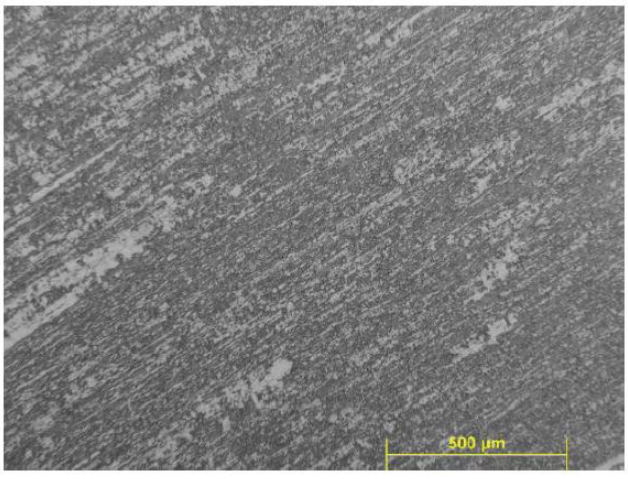

Fig. 1 Microstructure of the applied material

Table 1 Chemical composition of LDX2205

Element	C	Cr	Mn	Mo	N
m/m%	0.022	22.685	1.354	3.220	0.167
Element	Ni	P	S	Si	
m/m%	5.430	0.025	0.001	0.341	

Table 2 Mechanical properties of LDX2205

	R_m (MPa)	$R_{p0.2}$ (MPa)	A_{80} (%)
Value	887	718	29

2.1 Disk compression test

The Disk Compression Test (DCT) is an unconventional, non-standardized material-testing technique used to determine the biaxial anisotropy coefficient. The DCT methodology is based on the deformation of the disks under axial compression. The initial shape of the specimen was circular, with a nominal diameter of 8 mm and a nominal thickness of 1 mm. The specimens were manufactured from a sheet metal by laser cutting. The heat-affected zone was neglected. The HAZ thickness was measured at multiple locations and was found to be less than 0.08 mm. Both sides of the specimens were measured, and the minor difference observed was attributed to the nature of the laser-cutting process. It was found to be insignificant (~0.1 mm in diameter). Therefore, to ensure consistency, the same side of the specimens was measured throughout, making the deformation results comparable. The higher the anisotropy of the sheet metal, the more pronounced the elliptical shape of the compressed disks became. The value of r_b can be determined from the final shape of the compressed disks. Fig. 2 shows the test concept.

The compression was performed between two polished pressure plates; during the tests, force was measured, and crosshead displacement was recorded. The compression speed was set to 0.25 mm/min.

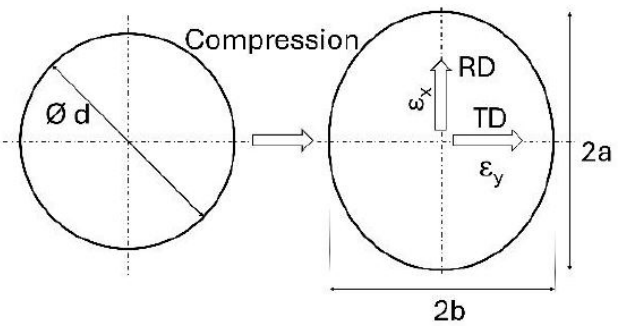

Fig. 2 Schematic drawing of the DCT specimen

The rolling direction (RD) is the major axis, and the transverse direction (TD) is the minor axis of the formed ellipses due to the anisotropy of the sheet metal. Sheets that were annealed after rolling show little or no anisotropy; therefore, in those cases, the shape of the final disk remains circular with a bigger diameter, and the value of r_b is close to 1. The notation of Fig. 2 shows the directions of the main strains in the plane (ε_x and ε_y). The third strain, ε_z, corresponded to the thickness strain due to compression. The sum of these three measured strains, according to volume constancy, Eq. (1), can be considered zero. However, measurement errors can lead to deviations from the hypotheses.

$$\varepsilon_x + \varepsilon_y + \varepsilon_z = 0\,. \tag{1}$$

The strains can be calculated as follows, using the notation of Fig. 2:

$$\varepsilon_x = \ln\left(\frac{2a}{d}\right) \tag{2}$$

$$\varepsilon_y = \ln\left(\frac{2b}{d}\right) \tag{3}$$

$$\varepsilon_z = \ln\left(\frac{h}{h_0}\right) \tag{4}$$

From the two planar (x and y – Eqs. (2) and (3), respectively) strains, the rb can be calculated according to Eq. (5) as the ratio of the transverse (y) and rolling direction (x) strains.

$$r_b = \frac{\varepsilon_y}{\varepsilon_x} \tag{5}$$

A total of 18 specimens were compressed: nine for lubricant comparison, three for load-driven experiments, and six for gradually loaded experiments.

2.2 Effect of friction on deformation

Firstly, the effect of the frictional conditions was taken into account. Three different greases were tested on three specimens, respectively. In theory, with the lowest friction during the tests, the highest strains occurred due to uninhibited deformation. The three lubricants were grease for high-pressure applications (grease), grease with graphite (graphite), and Teflon sheets with a thickness of 0.5 mm (PTFE).

The specimens were compressed with different lubricants at a maximum load of 110 kN on an Instron 8501 universal hydraulic material testing machine without stopping during the compression tests. A total of 9 specimens were tested using this method. After the tests, the specimen geometries were observed under an Olympus SZX16 stereomicroscope, and images were captured for image correlation analysis to determine the axes of the formed ellipses. Based on the measured parameters, the specimens greased with PTFE sheets performed best in terms of deformation, i.e., the compressed specimens exhibited more pronounced elliptical deformation (Fig. 3). Therefore, for the subsequent tests, PTFE sheets were used to reduce friction and achieve the maximum possible deformation.

Fig. 4 shows the three original and compressed disk specimens with the usage of PTFE lubricant. As can be observed visually, the deformation was significant, and the shapes were pronounced ellipses.

2.3 Load-driven compressions

Secondly, the specimens were gradually loaded from 50 kN to 100 kN with a load increment of 10 kN. In total, 6 specimens were compressed; at each load level, only one was.

2.4 Gradually loaded specimens

Thirdly, the specimens were compressed in increments of 10 kN. The first stop was set to 50 kN; between each stop, a photo of the actual geometry was taken for DIC analysis, and the specimens were compressed further. The PTFE sheets were renewed at every step. The maximum load was set to 100 kN. At each load level, three specimens were tested with this method. The height of the specimens was measured before and after compression in every case.

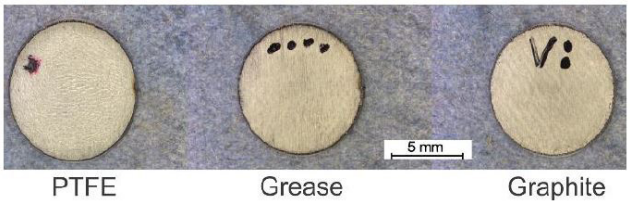

Fig. 3 Compressed specimens with the usage of different lubricants

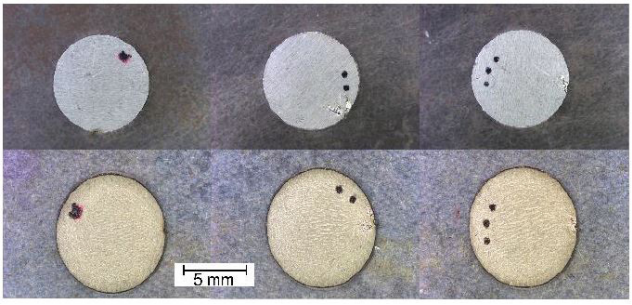

Fig. 4 Comparison of the compressed sheets before and after compression with the PTFE lubricant

2.5 Hardness testing

Hardness was measured with 500 g using the Buehler Indentamet 1100 microhardness testing machine with the indentation time of 11 s. The hardness was measured at least 9 points on each of the investigated specimens and then averaged. In the case of a fully compressed PTFE-lubricated one, the measurement was done along the major and minor axes.

3 Results and discussion

The measured force-displacement curves are presented in Fig. 5 for all lubricant cases.

In the case of the PTFE lubrication, the shapes of the curves differed from the other two measured cases, since a part of the curve is the compression of the PTFE sheets, although the slope of the curves was highly similar above ~45 kN force in all three cases.

The photos of the non-compressed and compressed disks were digitally measured using ImageJ [19] (Fig. 6).

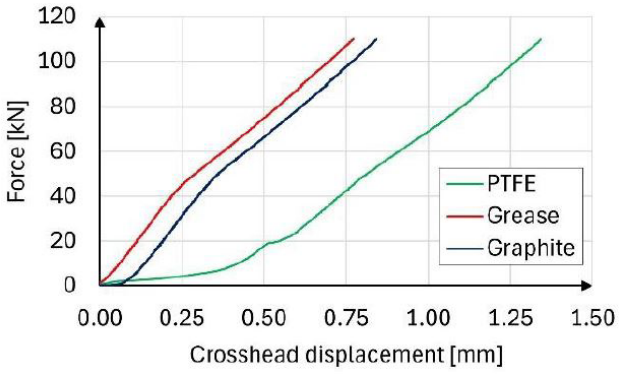

Fig. 5 Force-displacement curves – different lubricants

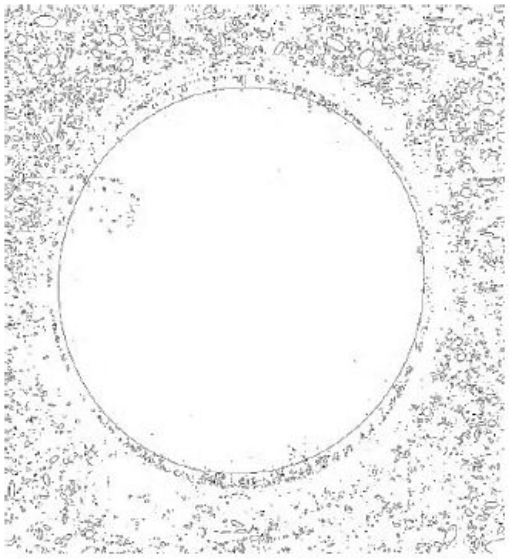

Fig. 6 Fitted ellipse (Specimen ID: 1)

The software can analyze photos and fit an ellipse to the edges of the specimen. The procedure yielded the major and minor axes of the ellipses, which can be used to determine the strains.

The non-deformed specimens were analyzed similarly; however, because they were considered perfectly circular, minor differences were observed. The initial diameter of the specimens was set as the average of the major and minor axes of the measured data. According to the DIC analysis, the average initial diameter of the specimens was 7.7 ± 0.13 mm, with an average roundness of 0.974 or an average aspect ratio of 1.026. From the initial diameter and the axes of the deformed ellipsoidal shape, the strains can be calculated according to Eqs. (2) and (3), respectively.

Fig. 7 shows the calculated strain distributions for differently lubricated specimens. The diagram shows that the strain values were lower with the Grease lubricant than in the other two cases, and the resulting data points showed significant deviation. In contrast with graphite, the values showed less deviation from each other, although the data points lay close to the isotropic deformation line. These observations implied that these lubricants were insufficient to determine the biaxial anisotropic coefficient of LDX2205 steel. The possible explanation was that the lubrication did not reduce the friction between the pressure plate and the disks enough to deform properly at a given load level. The third, PTFE lubrication, on the contrary, showed good correlation between the resultant point and a noticeably anisotropic deformation. The distribution of data points showed a pronounced deformation in the rolling direction (RD), with points lying below the line of isotropic deformation, indicating that the sheet was much more prone to deformation in this direction.

The load-driven experiments showed a clear deviation from isotropic deformation (Fig. 8). The fitted trendline passed through the origin because the available sheet

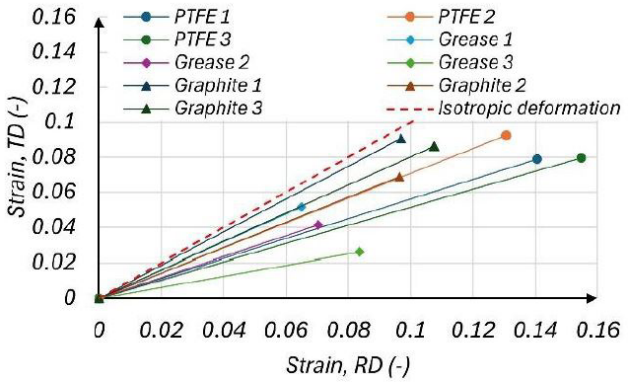

Fig. 7 Strain plots of the differently lubricated specimens (110 kN)

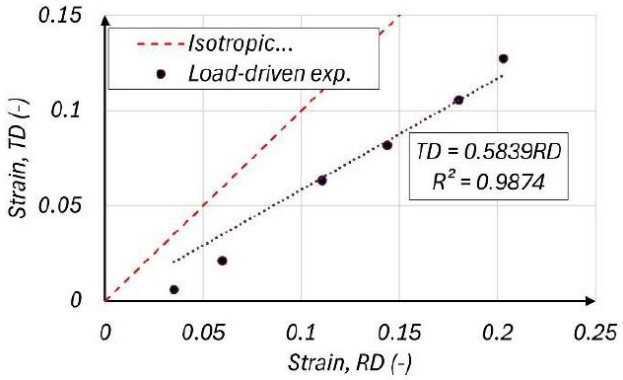

Fig. 8 Data plot of load-driven experiments (PTFE)

metal was treated as a zero state, with every subsequent deformation step relative to this point. Furthermore, the three testing methods were comparable. The coefficient of the fitted line was the biaxial anisotropy coefficient, in this case $r_b = 0.5839$.

The results from the gradually loaded specimens showed a less uniform distribution. The specimens (ID #17, #18, and #19) were measured gradually, and linear fits of the individual measurements were performed, as well as a fit of all the measurements. As shown in Fig. 9, the factors were different.

The fitted data varied across different sets of measurements. The *Gradually loaded - all* data set contains all the measured data and is in good agreement with the average of the individual data fits. The average value of the individual fits was $r_{b\_avg} = 0.5175$, i.e., the average of the coefficients for #17, #18, and #19, and the fitted value across all measurement data, which consists of the values from all three measurement series, was $r_b = 0.4978$, which were quite close to each other. However, the results differed from the load-driven experiments. The three sets of experiments showed that the r_b parameter is scattered. This phenomenon could be a sign of uneven frictional behavior due to the renewal of the PTFE sheets between load levels, or it may indicate that the specimens were not placed in the same fixed position.

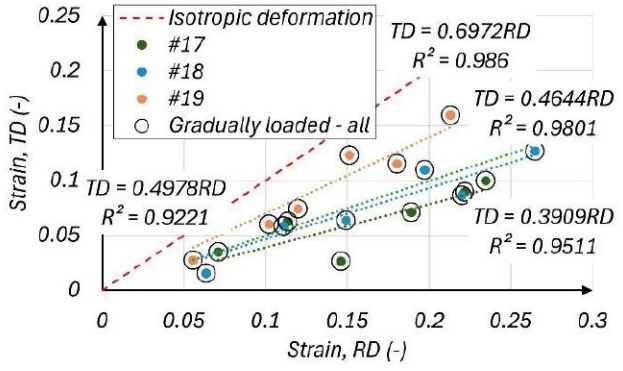

Fig. 9 Data plots of gradually loaded experiments (PTFE)

The results show that the PTFE is the most reliable lubricant among the investigated ones, and the load-driven method provides a more consistent dataset than the gradually loaded one.

The residual thickness was measured during the tests. Fig. 10 shows the average reduction of the disk's height. Each specimen was measured three times at each load increment. The diagram also contains the averaged heights of the initial and fully compressed specimens, totaling 24 measurements. The fitted equation is a second-order polynomial, which shows a very good fit, though it is close to a linear fit; therefore, the trend line is only for visual purposes.

The evaluation of volume constancy based on strains is shown in Table 3.

According to the assumption of volume constancy, the strain values should be equal to zero (Eq. (1)). However, the sum of the strains in the three principal directions is not exactly zero, indicating minor imperfections in the initial geometry and expected measurement uncertainties.

The hardness of the specimens was measured on fully loaded specimens. Table 4 contains the averaged microhardness values. The hardening behavior is clearly

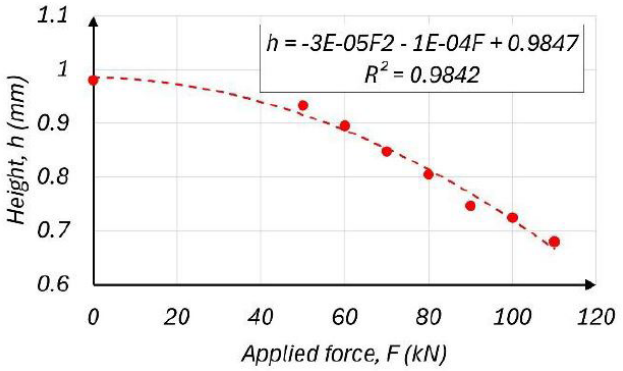

Fig. 10 Height reduction of the specimens

Table 3 Volume Constancy Assessment in DCT

Load (N)	$t_{avg.}$ (mm)	ε_{x_RD} (-)	ε_{y_TD} (-)	$\varepsilon_{z\_thickness}$ (-)	Sum of strains (-)
0	0.98	0.000	0.000	0.000	0.000
50	0.93	0.064	0.026	−0.049	0.041
60	0.90	0.109	0.060	−0.090	0.079
70	0.85	0.138	0.055	−0.145	0.048
80	0.80	0.189	0.099	−0.197	0.090
90	0.75	0.198	0.100	−0.272	0.026
100	0.72	0.238	0.129	−0.302	0.064

Table 4 Results of hardness testing

Specimen:	Initial	PTFE	Grease	Graphite
HV0.5	288.9	385.5	364.3	364.7

observed. The grease and graphite lubricants show almost identical values; the PTFE shows a slightly higher value.

The hardness values measured along the major and minor axes of a fully compressed PTFE-lubricated specimen are shown in Fig. 11. The origin of the diagram is located at the center of the deformed disk. The hardness distribution shows a maximum at the center of the specimen and decreases towards the edges; this can be observed on both axes. Although there are some local fluctuations, the trend remains similar. The distribution trends suggest the material flow was not perfectly uniform; however, no significant directional dependence can be identified.

The microstructure evolution is shown in Fig. 12, where the disks' actual deformation at different load levels was compared with the original, as-delivered state of the sheet metal. It is clearly visible that, for the applied 50 kN and 90 kN, the structure changes.

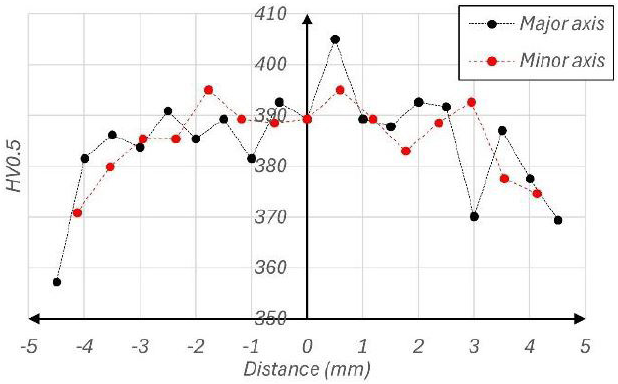

Fig. 11 Hardness distribution along the major and minor axes

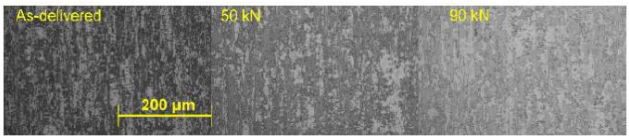

Fig. 12 Microstructures of gradually loaded specimens

Around the perimeter of the specimens, a more visible difference can be observed (Fig. 13) between the as-delivered condition and the compressed ones.

4 Summary

The disk compression test (DCT) was applied to determine the biaxial anisotropy coefficient (r_b) of LDX2205 duplex stainless steel. The aim of the study was to determine the biaxial anisotropy coefficient of the LDX 2205 type of DSS. Although the proper testing procedure and lubrication were unknown. The focus was on determining the proper frictional behavior and testing scheme; therefore, three different types of lubricants were used, and three methods were used to determine the most effective approach for this application. The tests showed that the application of PTFE sheets resulted in much less friction than the other two lubricants, as it produced the most pronounced elliptically shaped deformed specimens. Despite the gradually loaded specimens showing slightly lower values (r_b = 0.50-0.52) than those from the load-driven method (r_b = 0.58), the load-driven specimens were more realistic, as the method yielded the most consistent results. The hardness and microstructure analyses confirmed that the PTFE lubrication was the most appropriate choice for this test. Further investigation is needed to determine the scatter in the load-driven method, the effects of PTFE sheet thickness, and the effects of specimen size and shape.

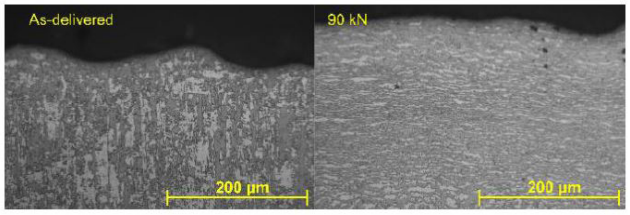

Fig. 13 Microstructures of gradually loaded specimens - perimeter

References

[1] Tisza, M. "Numerical modelling and simulation in sheet metal forming", Journal of Materials Processing Technology, 151(1–3), pp. 58–62, 2004. https://doi.org/10.1016/j.jmatprotec.2004.04.009

[2] Said, L. B., Kamoun T., Mars, J., Alharbi, S., Rajhi, W., Turki, M., Wali, M. "Data-driven deep drawing optimization: Response surface methodology and machine learning", Journal of Engineering Research, 14(1), pp. 595–605, 2025. https://doi.org/10.1016/j.jer.2025.10.010

[3] Yang, X., Yan, Y., Yang, H., Ma, J., Yi, L., Li, H. "Earing prediction in deep drawing of AA6016-T4 sheet: influences of element types, constitutive models and friction coefficients", International Journal of Lightweight Materials and Manufacture, 2026. https://doi.org/10.1016/j.ijlmm.2026.05.001

[4] Huan, T., Xing, A., Yang, F. Zhang, C., Xiang, N., Song, K. Zhang, W. "Anisotropic behavior and mechanism in electropulsing-assisted deep drawing of Ti/al laminated composite cups", Journal of Materials Research and Technology, 41, pp. 2807–2829, 2026. https://doi.org/10.1016/j.jmrt.2026.01.130

[5] Barlat, F., Brem, J. C., Yoon, J. W., Chung, K., Dick, R. E., Lege, D. J., Pourboghrat, F., Choi, S.-H., Chu, E. "Plane stress yield function for aluminum alloy sheets—part 1: theory", International Journal of Plasticity, 19(9), pp. 1297–1319, 2003. https://doi.org/10.1016/S0749-6419(02)00019-0

[6] Béres, J. G., Weltsch, Z., Borbély, R., Kölüs, L. M., Lukács, Zs. "An extended stress-based forming limit diagram focusing on the wrinkling phenomenon and the effect of the normal pressure on clamped surfaces", Journal of Materials Processing Technology, 322, 118196, 2023. https://doi.org/10.1016/j.jmatprotec.2023.118196

[7] Dick, E. R., Yoon J. W. "Plastic anisotropy and failure in thin metal: Material characterization and fracture prediction with an advanced constitutive model and polar EPS (effective plastic strain) fracture diagram for AA 3014-H19", International Journal of Solids and Structures, 151, pp. 195–213, 2018. https://doi.org/10.1016/j.ijsolstr.2018.03.008

[8] Anderson, N., Brown, D., McMurray, R. J., Leacock, A. G. "The influence of uniaxial prestrain on biaxial r-values in 7075-O aluminium alloy", AIP Conference Proceedings, 1353(1), pp. 1435–1440, 2011. https://doi.org/10.1063/1.3589718

[9] Martínez, A., Miguel, V., Coello, J., Manjabacas, M. C. "Determining stress distribution by tension and by compression applied to steel: Special analysis for TRIP steel sheets", Materials and Design, 125, pp. 11–25, 2017. https://doi.org/10.1016/j.matdes.2017.03.079

[10] Aretz, H., Barlat, F. "Influence of Contact Friction on the Experimental Determination of the Balanced Biaxial Strain-Ratio Using the Disc Compression Test", Key Engineering Materials, 611–612, pp. 529–535, 2014. https://doi.org/10.4028/www.scientific.net/KEM.611-612.529

[11] Camberg, A. A., Tröster, T. "A simplified method for the evaluation of the layer compression test using one 3D digital image correlation system and considering the material anisotropy by the equibiaxial Lankford parameter", IOP Conference Series: Materials Science and Engineering, 967, 012077, 2020. https://doi.org/10.1088/1757-899X/967/1/012077

[12] Tian, H., Brownell, B., Baral, M., Korkolis, Y. P. "Earing in cup-drawing of anisotropic Al-6022-T4 sheets", International Journal of Material Forming, 10(3), pp. 329–343, 2016. https://doi.org/10.1007/s12289-016-1282-y

[13] Mapelli, C., Barella, S., Mombelli, D., Baldizzone, C., Gruttadauria, A. "Comparison between symmetric and asymmetric hot rolling techniques performed on duplex stainless steel 2205", International Journal of Material Forming, 6(3), pp. 327–339, 2013. https://doi.org/10.1007/s12289-011-1089-9

[14] Reddy, M. S., Singaravelu, D. L., Narayanan, C. S. "Incremental Sheet Forming of Duplex Stainless Steel; Effect of Microstructure and Texture Evolution on Tensile Behavior", Journal of The Institution of Engineers (India): Series D, 106(3), pp. 2011–2020, 2025. https://doi.org/10.1007/s40033-024-00824-3

[15] Ranaa, R., Loiseauxb, J., Lahayec, C. "Microstructure, Mechanical Properties and Formability of a Duplex Steel", Materials Science Forum, 706–709, pp, 2271–2277, 2012. https://doi.org/10.4028/www.scientific.net/MSF.706-709.2271

[16] Pezzato, L., Gennari, C., Settimi, A. G., Kemény, A., Mészáros, I. "Effect of multi-pass cold rolling on the corrosion properties of 2101 duplex stainless steel", Metallurgia Italiana, 113(9), pp. 31–36, 2022.

[17] Varbai, B., Pickle, T., Májlinger, K. "Development and Comparison of Quantitative Phase Analysis for Duplex Stainless Steel Weld", Periodica Polytechnica Mechanical Engineering, 62(3), pp. 247–253, 2018. https://doi.org/10.3311/PPme.12234

[18] Varbai, B., Bolyhos, P., Kemény, D. M., Májlinger, K. "Microstructure and Corrosion Properties of Austenitic and Duplex Stainless Steel Dissimilar Joints", Periodica Polytechnica Mechanical Engineering, 66(4), pp. 344–349, 2022. https://doi.org/10.3311/PPme.21007

[19] National Institutes of Health (NIH) "ImageJ, (Version 1.54)", [computer program] Available at: https://imagej.nih.gov/ij/ [Accessed: 03 March 2026]